ET-SRCKF-Based Dynamic State Estimation for Cyber-Physical Distribution Systems With Delayed Measurements

Xiao Hu, *Graduate Student Member, IEEE*, Xinghua Liu, *Senior Member, IEEE*, Huaicheng Yan, *Senior Member, IEEE*, Gaoxi Xiao, *Senior Member, IEEE*, and Peng Wang, *Fellow, IEEE*

***Abstract*— This paper studies the dynamic state estimation problem for cyber-physical distribution systems (CPDSs) with false data injection attacks (FDIAs) and delayed measurements. In view of the characteristics of multiple measurement types, the equivalent current measurement transformation technique is adopted to make the measurement equation be expressed in the form of linear measurement model. Based on the mixed measurements of phasor measurement units (PMUs) and distribution remote terminal units (DRTUs), a novel model is constructed using Bernoulli distributed random variables to describe the delay phenomena. Further, in order to improve the transmission efficiency of the measurement data, an mechanism is introduced in the network transmission process to minimise the amount of data transmission in the network while ensuring the performance of system state estimation. A measurement model based on the event-triggered mechanism is developed, and an event-triggered square root cubature Kalman filter (ET-SRCKF) algorithm incorporating delayed measurements is designed to implement the state estimation of CPDSs, which can obtain the optimal estimation of the states under delayed measurements. Finally, simulated examples are conducted on the IEEE 33-bus test system, and the effectiveness of the proposed method is illustrated by numerical simulations.**

***Index Terms*— State estimation, event-triggered square root cubature Kalman filter, delayed measurements, equivalent measurements, cyber-physical distribution systems.**

I. Introduction

WITH the wide applications of information and communication technology in the distribution network, the cyber physical coupling in the distribution network is gradually deepened. A large number of data acquisition equipment, computer equipment and electrical equipment are connected through the power and the communication networks. The distribution network systems with the newly equipped characteristics of cyber-physical system (CPS) [1], [2], [3], [4], [5], [6], become the cyber-physical distribution systems (CPDSs) [7], [8], [9], [10]. The high dependence of the distribution network on the cyber system makes the physical system be inevitably prone to the information failure, delay, etc. Studies on how to handle such negative impacts therefore become a new hot topic.

State estimation is an important part of distribution automation system. With the massive access of distributed power supply and energy storage equipment, the operation mode of CPDSs becomes more flexible and complex than before which puts forward higher requirements for state estimation of CPDSs. Ensuring high accuracy and reliability of data is hence of particular importance [11], [12], [13], [14]. In order to achievehigher-precision measurement in CPDSs, the phasor measurement units (PMUs) are increasingly deployed. Different from DRTUs, the advanced PMUs are not only capable of directly measuring the voltage/current vector but also can be synchronized by GPS [15]. Despite their capabilities, the high installation cost prohibits PMUs from entirely replacing DRTUs in the foreseeable future. Hence, relying solely on PMUs cannot fulfill the observability requirements of distribution systems. A synergistic utilization of both DRTUs and PMUs is imperative to acquire comprehensive measurement information [16], [17], [18], [19]. In this paper, we shall consider the issues of data compatibility between the two types of measurement data.

Dynamic state estimation of CPDSs involves deriving optimal parameter estimates from data collected by measurement devices. This process aims to ascertain various parameters and operating states [20], to ensure the proper functioning of advanced applications such as subsequent static security analysis, fault isolation, and recovery. However, the increasing prevalence of cyber attacks poses a significant threat to power system security, potentially leading to severe consequences like loss of equipment control, power transmission interruptions, or grid collapse. False Data Injection Attacks (FDIAs) represent a prevalent cyber attack method capable

Manuscript received 6 September 2023; revised 31 December 2023; accepted 13 February 2024. This work was supported in part by the National Natural Science Foundation of China under Grant U2003110, in part by the Shaanxi Outstanding Youth Science Fund Project under Grant 2024JC-JCQN-68, and in part by the High Level Talents Plan of Shaanxi Province for Young Professionals. This article was recommended by Associate Editor T. Fernando. *(Corresponding authors: Xinghua Liu; Huaicheng Yan.)*

Xiao Hu and Xinghua Liu are with the School of Electrical Engineering, Xi'an University of Technology, Xi'an 710048, China (e-mail: hux@stu.xaut.edu.cn; liuxh@xaut.edu.cn).

Huaicheng Yan is with the School of Information Science and Engineering, East China University of Science and Technology, Shanghai 200237, China (e-mail: hcyan@ecust.edu.cn).

Gaoxi Xiao and Peng Wang are with the School of Electrical and Electronic Engineering, Nanyang Technological University, Singapore 639798 (e-mail: egxxiao@ntu.edu.sg; epwang@ntu.edu.sg).

Color versions of one or more figures in this article are available at https://doi.org/10.1109/TCSI.2024.3367173.

Digital Object Identifier 10.1109/TCSI.2024.3367173

of compromising remote terminal units, PMUs, or tampering with data transmitted from meters to control centers [21]. FDIAs can manipulate meter measurements, either by directly compromising devices or by tampering with the data reported to control centers. These attacks might introduce biases into the estimated state outputs [22], obscuring the actual operating state of the power grid. This obstruction prevents timely detection of the attacker's motives, potentially causing practical or economic repercussions for CPDSs. Therefore, investigating dynamic state estimation algorithms for CPDSs under the influence of FDIAs becomes crucial for enhancing system resilience and security.

In the measurement system, due to the FDIAs on the CPDSs, there are always random delays in the measurement data transmitted by the SCADA and PMU measurement systems, resulting in mixed measurement data being transmitted to the estimator that is not always up-to-date [23]. How to design a filtering algorithm for the dynamic state estimation of CPDSs with delayed measurements is a crucial research topic in engineering applications [24], [25], [26], [27], [28], [29]. Su and Lu [30] reported the earliest work considering time delay in power systems, which used a stochastic extended Kalman filter algorithm to provide an optimal estimate of state for a system where the measurements are randomly delayed. An adaptive Kalman filtering algorithm to handle lost or delayed measurement was addressed in [31]. A limitation of the existing work is that it assumes the whole measurement vector to be either received in time or delayed, which cannot describe the situation, where only partial information is delayed. In addition, Yang et al. [32] proposed a modified state estimator to solve the power system state estimation problem with time delay, which was based on the assumption that all measurement data are obtained from PMUs. However, few works are aimed at representing a state estimator with delayed measurements to handle the issue of mixed DRTU and PMU measurements. On the other hand, the existing studies on CPDSs state estimation rarely consider the impact of network transmission performance, and all assume that the transmission of measured data is not limited by network bandwidth.

However, the transmission of large amounts of data causes packet loss and delay [33], [34], which will adversely affect the performance of state estimation in practical applications. On the basis of ensuring the estimated performance of the system, the network data transmission volume is reduced as much as possible. Event triggering mechanism can effectively reduce redundant data transmission in the network [35], [36], [37], [38]. Motivated by the previous discussions, the goal of this paper is to design an algorithm based on SRCKF and capable of handling mixed PMU, DRTU and one-step delay measurements. In order to reduce the data transmission of the measuring device and ensure the performance of state estimation, zero-input data retention strategy is adopted to establish a measurement model under event triggering mechanism. An ET-SRCKF with delay state estimation algorithm is proposed to solve the problem of mixing PMU and DRTU measurements. To conclude, the main contributions of this paper are extracted in the following aspects.

1) The compatibility problem of the two types of measurement data is solved by the equivalent current measurement transformation technique, which can improve the consistency of information and the accuracy of state estimation.
2) The ET-SRCKF algorithm based on delay measurement is designed not only to ensure the state estimation accuracy but also to reduce the amount of data transmission and alleviate the pressure of CPDSs communication.
3) In contrast to the state estimation methods of [27] and [28], the proposed method has better estimation performance, and the algorithm is robust to partial measurement delays and effective in handling both PMU and DRTU measurements [32].

Notation: Throughout the entire article, $\mathbb{R}$ is the n-dimensional Euclidean space. $E[w]$ is utilized to represent the expectation of a variable w. $y \in \mathbb{R}^n$, $\|y\|$ denotes the L_2 norm of vector y. A^T indicates the transpose of matrix A. diag{...} means the block-diagonal matrix. $N(\mu, R)$ is used to describe the Gaussian stochastic process, where μ and R are the mean value and covariance matrix of the Gaussian stochastic process, respectively.

II. Problem Formulation and Preliminaries

A. Mathematical Model of CPDS State Estimation

In this paper, the system state $x_k \in \mathbb{R}^n$ is defined as the real and imaginary parts of bus voltage in the CPDS, that is, $x_k = \left[x_{1,k}, \ldots, x_{l,k}, \ldots, x_{d,k}\right]^T$, where $x_{l,k} = \left[x_{l,k,re}, x_{l,k,im}\right]$ is a vector representing the state of bus l at time instant k. Then, the state space model of the system can be described as

$$x_k = f(x_{k-1}) + w_k, \tag{1}$$

where $f(\cdot)$ is the state equation, respectively. w_k represents uncorrelated white Gaussian noise.

According to Holt-Winters double exponential smoothing method [14], the state equation can be updated as follows

$$\begin{cases} \hat{x}_{k|k-1} = S_{k-1} + b_{k-1}, \\ S_{k-1} = \alpha_H \hat{x}_{k-1|k-1} + (1-\alpha_H)\hat{x}_{k-1|k-2}, \\ b_{k-1} = \beta_H (S_{k-1} - S_{k-2}) + (1-\beta_H) b_{k-2}, \end{cases} \tag{2}$$

where $\hat{x}_{k|k-1}$ is the predicted value of the system status. S_{k-1} and b_{k-1} are the horizontal component and vertical component at $k-1$ moment respectively. α_H and β_H are called the smoothing index, and their value range is usually $(0, 1)$.

Generally, the DRTU measurement vector $z_k^{drtu} \in \mathbb{R}^{m1}$ is obtained by $z_k^{drtu} = \left[P_k^{fT}, Q_k^{fT}, P_k^T, Q_k^T\right]^T$, where P_k and Q_k are the vectors of the real and reactive power injections at all buses, and P_k^f and Q_k^f are the vectors of the real and reactive power flows between all buses, respectively.

Then, similar to [5], the measurement vector $z_{l,k}^{drtu}$ from the DRTU at bus l is derived

$$\begin{aligned} P_l^f \triangleq P_{ij}^f &= -(x_{i,re}x_{j,re} + x_{i,im}x_{j,im})g_{ij} \\ &\quad \times (x_{i,re}^2 + x_{i,im}^2)g_{ij} - (x_{i,im}x_{j,re} - x_{i,re}x_{j,im})b_{ij}, \\ Q_l^f \triangleq Q_{ij}^f &= (x_{i,re}x_{j,im} - x_{i,im}x_{j,re})g_{ij} \\ &\quad - (x_{i,re}^2 + x_{i,im}^2)b_{ij} + (x_{i,re}x_{j,re} + x_{i,im}x_{j,im})b_{ij}, \end{aligned}$$

$$\begin{aligned} P_l &= x_{l,re}\sum_{j\in B_l}(G_{lj}x_{j,re}-B_{lj}x_{j,im}) \\ &\quad + x_{l,im}\sum_{j\in B_l}\left(G_{lj}x_{j,im}+B_{lj}x_{j,re}\right), \\ Q_l &= x_{l,im}\sum_{j\in B_l}(G_{lj}x_{j,re}-B_{lj}x_{j,im}) \\ &\quad - x_{l,re}\sum_{j\in B_l}(G_{lj}x_{j,im}+B_{lj}x_{j,re}), \end{aligned} \tag{3}$$

where $G_{lj}+jB_{lj}$ is used to indicate the ljth term of the complex admittance connected to bus l. $g_{ij}+jb_{ij}$ denotes the series admittance between bus i and bus j. B_l is a set of the number of buses connected to bus l.

The DRTU measurement vector $z_{l,k}^{drtu}$ is modeled as the following equation

$$z_k^{drtu} = \eta(x_k) + v_{1,k} \tag{4}$$

where $\eta(x_k)$ is obtained by Eq. (3), $v_{1,k}$ is the DRTU measurement noise, which satisfies the Gaussian distribution $N(0,\sigma_c^2)$.

In order to solve the problem of the difference of data components obtained by different measuring devices, we employ the measurement transformation technology to convert the measurement collected by DRTUs into the equivalent measurement of the real part and imaginary part of the node injection current, as well as the measurement of the real part and imaginary part of the branch current. It is noticed that if all measured quantities are voltage or current phasors and the states to be estimated are bus voltages, then the linear measurement model is obtained in [36].

For P_l and Q_l, the equivalent current injection at the same bus is obtained from

$$\begin{aligned} I_{l,re} &= \frac{P_l x_{l,re}+Q_l x_{l,im}}{x_{l,re}^2+x_{l,im}^2}, \\ I_{l,im} &= \frac{P_l x_{l,im}-Q_l x_{l,re}}{x_{l,re}^2+x_{l,im}^2}. \end{aligned} \tag{5}$$

Similarly, for P_{lj} and Q_{lj}, the equivalent branch current is obtained from

$$\begin{aligned} I_{lj,re} &= \frac{P_{lj}x_{l,re}+Q_{lj}x_{l,im}}{x_{l,re}^2+x_{l,im}^2}, \\ I_{lj,im} &= \frac{P_{lj}x_{l,im}-Q_{lj}x_{l,re}}{x_{l,re}^2+x_{l,im}^2}. \end{aligned} \tag{6}$$

The measurement vector $z_l^{pmu}\in\mathbb{R}^{m2}$ from the PMU is detailed as $z_l^{pmu}=[V_{i,re}^{pmu}, V_{i,im}^{pmu}, I_{ij,re}^{pmu}, I_{ij,im}^{pmu}]^T$.

Similarly, based on the power flow calculation, each item of the above measurement vector with PMUs can be described

$$\begin{cases} I_{ij,re}^{pmu} = x_{i,re}g_{ij} - x_{i,im}b_{ij} - x_{j,re}g_{ij} + x_{j,im}b_{ij}, \\ I_{ij,im}^{pmu} = x_{i,im}g_{ij} + x_{i,re}b_{ij} - x_{j,im}g_{ij} - x_{j,re}b_{ij}, \\ V_{i,re}^{pmu} = x_{i,re}, \\ V_{i,im}^{pmu} = x_{i,im}. \end{cases} \tag{7}$$

The PMU measurement vector z_k^{pmu} can be expressed as

$$z_k^{pmu} = \mathcal{L}(x_k) + v_{2,k} \tag{8}$$

where $v_{2,k}$ is the noise from the PMU measurement, which satisfies the Gaussian distribution $N(0,\sigma_p^2)$.

Due to the equivalent measurements used instead of the actual ones in state estimation, the error propagation theory is required to evaluate the equivalent measurement's error covariance. For instance, the standard deviation of the equivalent current flow σ_{Ic}^2 is obtained from

$$\sigma_{Ic}^2 = \frac{\sigma_c^2}{x_{re}^2+x_{im}^2} \tag{9}$$

where σ_c is the standard deviation of DRTUs, x_{re} and x_{im} are the real and imaginary parts of the state vector, respectively. Details of the equivalent measurements and the corresponding error covariance can be seen in [19].

Finally, combining with Eq. (5)- Eq. (7), the mixed measurement equation of CPDS can be summarized as

$$z_k = Hx_k + v_k \tag{10}$$

where $z_k = [I_{l,re}, I_{l,im}, I_{ij,re}, I_{ij,im}, z_l^{pmu}]^T \in \mathbb{R}^m$, v_k is the measurement error vector. Notice that different types of standard deviations are independent of each other. Jacobian matrix H_i can be expressed as

$$H_i = \begin{bmatrix} \partial I_{i,re}/\partial x_{i,re} & \partial I_{i,re}/\partial x_{i,im} \\ \partial I_{i,im}/\partial x_{i,re} & \partial I_{i,im}/\partial x_{i,im} \\ \partial I_{ij,re}/\partial x_{i,re} & \partial I_{ij,re}/\partial x_{i,im} \\ \partial I_{ij,im}/\partial x_{i,re} & \partial I_{ij,im}/\partial x_{i,im} \\ \partial I_{ij,re}^{pmu}/\partial x_{i,re} & \partial I_{ij,re}^{pmu}/\partial x_{i,im} \\ \partial I_{ij,im}^{pmu}/\partial x_{i,re} & \partial I_{ij,im}^{pmu}/\partial x_{i,im} \\ \partial V_{i,re}/\partial x_{i,re} & 0 \\ 0 & \partial V_{i,im}/\partial x_{i,im} \end{bmatrix}.$$

Remark 1: In this paper, the time synchronization caused by different sampling instants and refreshing rates of PMU and DRTU data is not considered when solving the data compatibility problem. Since the system is assumed unchangeable during the scan for measurement, the synchrinization issues can be ignored under steady-state operations.

B. False Data Injection Attacks Model

In the field of research on the detection of bad data against the CPDSs, experts and scholars have achieved considerable achievements. A variety of effective detection methods have been proposed, yet most of them are still based on residuals analysis [15].

$$r = z_k - \hat{z}_k \tag{11}$$

where $\hat{z}_k$ represents the estimated vector of z_k.

According to the definition of the residual, Eq. (10) can be rewritten as follows [20]:

$$r = z_k - H\hat{x}_k \tag{12}$$

The measurement vector containing false data is defined as $z_a = z_k + a$, where $z_k = [z_1,\ldots,z_m]^T$ is the original measurement vector and $a = [a_1,\ldots,a_n]^T$ is the false data vector injected into the measurement. The state quantity after

the attack can be expressed as $\hat{x}_a = \hat{x}_k + c$, where $c = [c_1, \ldots, c_n]^T$ is the arbitrary nonzero error vector of the state quantity caused by FDIAs. The residuals after attacks can be calculated as follows

$$\begin{aligned} \|r\| &= \left\|z_a - H\hat{x}_a\right\| \\ &= \|z_k + a - H(\hat{x}_k + c)\| \\ &= \|z_k - H\hat{x}_k + a - Hc\| \end{aligned} \tag{13}$$

If the attack vector meets $a = Hc$, the following formula is true.

$$\|r\| = \left\|z_a - H\hat{x}_a\right\| = \|z_k - H\hat{x}_k\| \tag{14}$$

Eq. (14) suggests that the residual values before and after the FDIAs are equal, and then the residual-based bad data detection is unable to identify the false data. Consequently, the FDIAs are successfully applied to the measurement vector when the attack is modelled as $a = Hc$. In this case, the measurement vector under the attack has a larger deviation from the true vector, which will undermine the safe and stable operation of CPDSs [28].

In [29], If the errors of attack vectors are taken into account, the residual values before and after the FDI attacks are not equal. Then the following formula is obtained

$$\begin{aligned} \left\|z_a - H\hat{x}_a\right\| &= \|z_k - H\hat{x}_k + a - Hc\| \\ &\le \|z_k - H\hat{x}_k\| + \|a - Hc\| \end{aligned} \tag{15}$$

However, if the residual value of the measurement data is less than the detection threshold in the detection process, the FDIAs are still successfully hidden. Furthermore, the detection threshold J is determined by superimposing a certain redundancy on the normal maximum estimated deviation. The formula of the detection is as follows

$$\|z_k - H\hat{x}_k\| \le \left\|z_a - H\hat{x}_a\right\| \le J \tag{16}$$

Thus, if z_a satisfies Eq. (15), the FDIAs can be implemented to the CPDSs.

Remark 2: The basic principle of residuals analysis is illustrated below. Under the circumstance of ignoring noise and assuming that all state quantities are mutually independent and the measurement obeys the normal distribution, the residuals obey the chi-square distribution which the maximal degree of freedom is $m - n$. Set an appropriate threshold J, the size of which is determined by the level of significance. If $||r|| < J$, it is considered that there is no false data injection attacks. Otherwise, it means FDIAs exist. FDIAs make full use of the vulnerability of this detection mechanism. The attackers construct the well-designed attack vector to keep the residuals unchanged before and after the attack, in which case they can avoid detection.

In practice, due to limited bandwidth issues and long-distance communication, delays will inevitably occur in the measurement data transmitted from DRTUs and PMUs, which leads to the mixed measurement being transmitted to the estimator not always to be updated. In this paper, the hybrid measurement model with one-step stochastic delay is considered. In [39], the delayed measurement equation is always described as follows

$$y_{d,k} = (I - \zeta_k)z_k + \zeta_k z_{k-1} \tag{17}$$

where $\zeta_k = \text{diag}\{\zeta_{1,k}, \zeta_{2,k}, \ldots, \zeta_{m,k}\}$ is the measurement delay matrix, ς and $\varsigma(I - \varsigma)$ are its mean and variance. The ith element $\zeta_{i,k}$ is a stochastic variable, which satisfies the Bernoulli distribution that takes the possible value on $\{0, 1\}$. Furthermore, we define

$$\begin{cases} P(\zeta_{i,k} = 1) = E[\zeta_{i,k}] = \varsigma_i, \\ P(\zeta_{i,k} = 0) = 1 - E[\zeta_{i,k}] = 1 - \varsigma_i, \\ E[(\zeta_{i,k} - \varsigma_i)^2] = (1 - \varsigma_i)\varsigma_i, \end{cases} \tag{18}$$

where ς_i is called the measurement delay rate of the ith measurement. ζ_k is uncorrelated with $v_{1,k}$, $v_{2,k}$, and x_0. If ς_i = is not all equal to 0, only part of the mixed measurements are delayed.

Remark 3: In practice, due to the limited band-width and complex communication network, there is a certain probability that information transmitted by measurement data at one moment may arrive on time with a delay. Distinguished from [23], this partial delay measurement model is described by Eq. (17).

III. ET-SRCKF-Based State Estimation With Delayed Measurements

A. Predicting

In the SRCKF algorithm, L represents the number of cubature points, $L = 2n$ for third degree spherical-radial cubature rule; the set of $2n$ cubature points is given by

$$\xi_i = \begin{cases} \sqrt{n}\mathbf{e}_i, & i = 1, 2, \ldots, n, \\ -\sqrt{n}\mathbf{e}_{i-n}, & i = n+1, n+2, \ldots, 2n, \end{cases} \tag{19}$$

where $\mathbf{e}_i$ denotes the ith column of a n-dimensional unit matrix.

The initial state estimated value and its error covariance matrix are given by

$$\hat{x}_0 = E(x_0),\ P_0 = E[(x_0 - \hat{x}_0)(x_0 - \hat{x}_0)^T] \tag{20}$$

The initial value S_0 of the square-root factor of error covariance matrix is computed by the Cholesky decomposition of P_0.

$$S_0 = (\text{chol}(P_0))^T \tag{21}$$

Evaluate cubature points and propagate them through the state function

$$\begin{cases} \chi_{i,k-1} = S_{k-1}\xi_i + \hat{x}_{k-1}, \\ \chi^*_{i,k|k-1} = f(\chi_{i,k-1}). \end{cases} \tag{22}$$

Estimate the predicted state

$$\hat{x}_{k|k-1} = \frac{1}{L}\sum_{i=1}^{L} \chi^*_{i,k|k-1} \tag{23}$$

Compute the square-root factor of predicted error covariance matrix

$$\begin{cases} \begin{bmatrix} A & B \end{bmatrix} = \mathrm{qr}\left(\begin{bmatrix} \chi^*_{k|k-1} & S_{Q,k-1} \end{bmatrix}^T \right), \\ S_{k|k-1} = B(1:n,:)^T, \end{cases} \tag{24}$$

where $S_{Q,k-1}$ is a square-root factor of Q_{k-1}, obtained by

$$S_{Q,k-1} = (\mathrm{chol}(Q_{k-1}))^T$$
$$\chi^*_{k|k-1} = \frac{1}{\sqrt{L}} \left[\chi^*_{1,k|k-1} - \hat{x}_{k|k-1}, \ldots, \chi^*_{L,k|k-1} - \hat{x}_{k|k-1} \right].$$

A and B are the unitary matrix and upper triangular matrix, respectively, through QR decomposition.

B. Filtering

Taking into account Eq. (17), the mean $\hat{y}_{d,k|k-1}$ and square-root factor of the innovation covariance matrix $S_{yy,k|k-1}$, as well as the cross-covariance $P_{xy,k|k-1}$ are formulated as

$$\begin{cases} \hat{y}_{d,k|k-1} = (I - \varsigma)\hat{z}_{k|k-1} + \varsigma \hat{z}_{k-1}, \\ S_{yy,k|k-1} = (I - \varsigma) S_{zz,k|k-1} + \varsigma S_{zz,k-1} \\ \qquad\qquad + \varsigma(I - \varsigma)(\hat{z}_{k|k-1} - \hat{z}_{k-1})(\hat{z}_{k|k-1} - \hat{z}_{k-1})^T, \\ P_{xy,k|k-1} = P_{xz,k|k-1}(I - \varsigma) + P_{xz,k-1}\varsigma. \end{cases} \tag{25}$$

As in the prediction step, the statistics of z_{k-1} are approximated from the cubature points $\chi_{i,k-1}$, by defining $\lambda^*_{i,k|k-1} = H\chi_{i,k-1}$, we have the following

$$\begin{cases} \hat{z}_{k-1} = \dfrac{1}{L} \displaystyle\sum_{i=1}^{L} \lambda^*_{i,k|k-1}, \\ \begin{bmatrix} A & B \end{bmatrix} = \mathrm{qr}\left(\begin{bmatrix} Z^*_{k-1} & \mathrm{S}_{R,k-1} \end{bmatrix}^T \right), \\ S_{zz,k-1} = B(1:m,:)^T, \\ P_{xz,k-1} = \chi_{k-1}(Z^*_{k-1})^T, \end{cases} \tag{26}$$

where $S_{R,k-1}$ is a square-root factor of R_{k-1}, obtained by

$$S_{R,k-1} = (\mathrm{chol}(R_{k-1}))^T,$$
$$Z^*_{k-1} = \frac{1}{\sqrt{L}} \left[\lambda^*_{1,k|k-1} - \hat{z}_{k-1}, \ldots, \lambda^*_{L,k|k-1} - \hat{z}_{k-1} \right],$$
$$\chi_{k-1} = \frac{1}{\sqrt{L}} \left[\chi_{1,k-1} - \hat{x}_{k-1}, \ldots, \chi_{L,k-1} - \hat{x}_{k-1} \right].$$

However, to approximate the statistics of z_k, which is a function of x_k, we use the information from the statistics given in Eqs. (23)-(24). The formulas are described as follows

1) Evaluate cubature points and update the propagated cubature points through the measurement function

$$\begin{cases} \chi_{i,k|k-1} = S_{k|k-1}\xi_i + \hat{x}_{k|k-1}, \\ Z_{i,k|k-1} = H\chi_{i,k|k-1}. \end{cases} \tag{27}$$

2) Estimate the predicted measurement

$$\hat{z}_{k|k-1} = \frac{1}{L} \sum_{i=1}^{L} Z_{i,k|k-1} \tag{28}$$

3) Compute the square-root factor of the innovation covariance matrix

$$\begin{cases} \begin{bmatrix} A & B \end{bmatrix} = \mathrm{qr}\left(\begin{bmatrix} Z^*_{k|k-1} & S_{R,k} \end{bmatrix}^T \right), \\ S_{zz,k|k-1} = B(1:m,:)^T, \end{cases} \tag{29}$$

where $S_{R,k}$ is a square-root factor of R_k, obtained by $S_{R,k} = (\mathrm{chol}(R_k))^T$ and

$$Z^*_{k|k-1} = \frac{1}{\sqrt{L}} [Z_{1,k|k-1} - \hat{z}_{k|k-1}, \ldots, \ldots, Z_{L,k|k-1} - \hat{z}_{k|k-1}].$$

4) Compute the cross-covariance matrix

$$P_{xz,k|k-1} = \chi_{k|k-1}(Z^*_{k|k-1})^T \tag{30}$$

where

$$\chi_{k|k-1} = \frac{1}{\sqrt{L}} [\chi_{1,k|k-1} - \hat{x}_{k|k-1}, \ldots, \ldots, \chi_{L,k|k-1} - \hat{x}_{k|k-1}].$$

The statistics of z_{k-1} and z_k are substituted in Eq. (25) to obtain those of $y_{d,k}$, which are used in the following equations providing the filter of x_k and the error covariance:

$$\begin{cases} \hat{x}_k = \hat{x}_{k|k-1} + K_k(y_{d,k} - \hat{y}_{d,k|k-1}), \\ \begin{bmatrix} A & B \end{bmatrix} = \mathrm{qr}\left(\begin{bmatrix} \chi_{k|k-1} - K_k Z^*_{k|k-1} & K_k S_{R,k} \end{bmatrix}^T \right), \\ S_k = B(1:n,:)^T, \end{cases} \tag{31}$$

where

$$K_k = (P_{xy,k|k-1}/{S_{yy,k|k-1}}^T)/S_{yy,k|k-1}.$$

C. Event-Triggered Mechanism

In the CPDSs state estimation, the data measured by the measuring device needs to be transmitted to the system state estimator through the network. With the increase of measuring device layout in CPDSs, the amount of measurement data transmitted by network is increasing, which will lead to the increase of communication channel pressure and network induction phenomenon. In order to rationally utilize communication resources and relieve the pressure of network communication, an event triggering mechanism is used in this paper to reduce the amount of data transmission from measuring device to estimator. As shown in Fig. 1, the CPDSs measurement data is obtained by the DRTU and PMU measurement devices. The event trigger controller filters the measurement data according to the event trigger conditions, and transmits the measured data meeting the conditions to the estimated value $\hat{x}_k$ of the CPDSs state at time k.

In order to reduce the data transmission amount of measuring device and ensure the performance of state estimation, distributed event triggering strategy is adopted in this paper because the distribution network has many points and wide areas and the state changes of nodes are not synchronized. The event trigger controller is integrated into the measuring device, and each event trigger controller

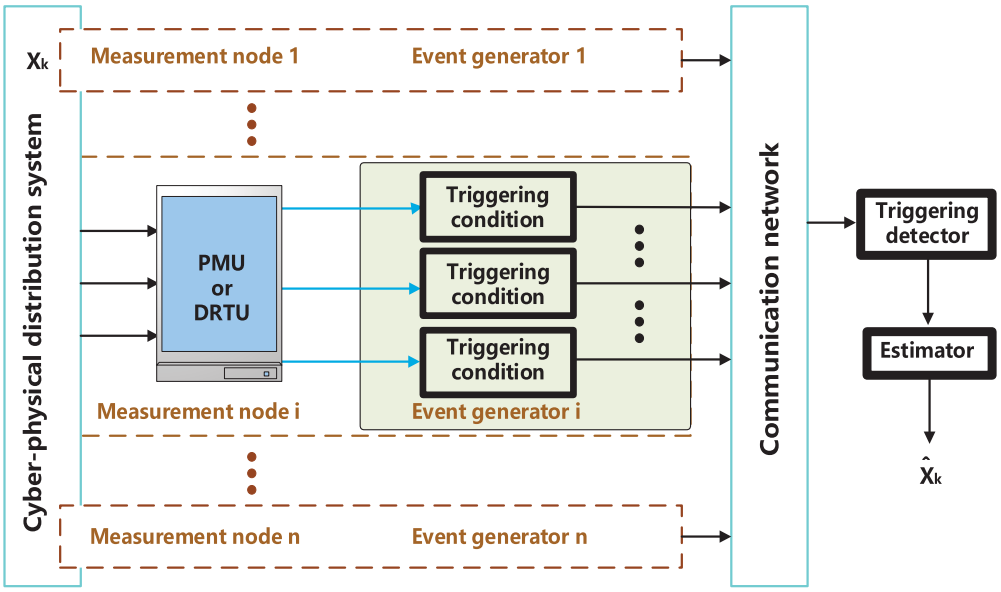

Fig. 1. State estimation with event-triggered mechanism in the cyber-physical distribution systems.

independently detects whether the data measured by the measuring device meets the trigger conditions.

First, given the event trigger threshold δ_i and the maximum number of sampling N_{max}, it is defined that $\varepsilon_{i,k} = z_{i,k} - z_{i,\tau}$ represents the difference between the measured data $z_{i,k}$ at time k of the ith measuring device and the measured data transmitted to the estimator at the nearest time, $z_{i,\tau}$. Event generation function is shown in the following Eq. (32)

$$l_i\left(\varepsilon_{i,k}, \delta_i\right) = \varepsilon_{i,k}^{\mathrm{T}}\varepsilon_{i,k} - \delta_i \tag{32}$$

where δ_i is the given event trigger threshold. Define the event trigger logic as

$$\gamma_{i,k} = \begin{cases} 1, & l_l\left(\varepsilon_{i,k}, \delta_i\right) \geq 0 \\ 0, & l_i\left(\varepsilon_{i,k}, \delta_i\right) < 0 \end{cases} \tag{33}$$

The value of $\gamma_{i,k}$ determines whether the measured data and $y_{i,k}$ will be transmitted to the estimator through the communication network. If $\gamma_{i,k} = 1$, the measured data will be transmitted to the estimator; otherwise, it will not be transmitted. At this time, the measurement data received by the time k estimator can be expressed as

$$\breve{z}_{i,k} = \begin{cases} z_{i,k}, & \gamma_{i,k} = 1 \\ 0, & \gamma_{i,k} = 0 \end{cases} \tag{34}$$

Remark 4: According to [40] and [41], the event-triggering scheme based on system outputs is subjected to attacks or external interference, which may lose efficacy under lack measurement information. In contrast, the proposed event-triggered mechanism remains operational under the conditions of DRTUs without sampled information, since the triggering threshold is set manually independent of the system output. It is worth mentioning that the event-triggering mechanism adopted in this paper can reduce computational complexity and exhibits lower conservatism.

D. SRCKF Algorithm Based on Event-Triggered Mechanism

In order to solve the problem of incomplete measurements received by the estimator due to the introduction of the event trigger mechanism, the ET-SRCKF algorithm based on the event trigger mechanism is proposed in this paper.

According to the zero-input data retention strategy, the measurement information transmitted to the estimator at time k is

$$\breve{z}_k = \Phi_k z_k \tag{35}$$

where $\Phi_k = \mathrm{diag}\left(\gamma_k^1 I_1, \ldots, \quad \gamma_k^i I_i, \ldots, \gamma_k^n I_n\right)$, where I_i is the identity matrix, whose dimension is equal to the dimension of the data measured by the ith measuring device.

By revising Eq. (27) and Eq. (28) according to Eq. (35), we can obtain

$$\begin{cases} \chi_{i,k|k-1} = S_{k|k-1}\xi_i + \hat{x}_{k|k-1}, \\ {Z^{et}}_{i,k|k-1} = \Phi_k Z_{i,k|k-1}. \end{cases} \tag{36}$$

$$\hat{z}_{k|k-1}^{et} = \Phi_k \hat{z}_{k|k-1} \tag{37}$$

where the superscript et represents the corresponding physical quantity under the event triggering mechanism, and the same is true below.

According to Eq. (29) and Eq. (30), the innovation covariance matrix and the cross-covariance matrix of ET-SRCKF algorithm can be obtained

$$P_{zz,k|k-1}^{et} = Z_{k|k-1}^{*et}(Z_{k|k-1}^{*et})^T + \Phi_k R_k \Phi_k + Q_k^{\mu} \tag{38}$$

where Q_k^{μ} is the given positive definite matrix to ensure the positive definiteness of the measurement covariance matrix under the event triggered data transmission mechanism.

$$P_{xz,k|k-1}^{et} = \chi_{k|k-1}(Z_{k|k-1}^{*et})^T \tag{39}$$

where

$$Z_{k|k-1}^{*et} = \frac{1}{\sqrt{L}}[Z_{1,k|k-1}^{et} - \hat{z}_{k|k-1}^{et}, \ldots, \\ \ldots, Z_{L,k|k-1}^{et} - \hat{z}_{k|k-1}^{et}].$$

Based on the previous derivation results, combined with the SRCKF algorithm framework, the ET-SRCKF algorithm can be obtained

$$\begin{cases} \hat{x}_k = \hat{x}_{k|k-1} + K_k^{et}(\breve{y}_{d,k} - \hat{y}_{d,k|k-1}^{et}), \\ \begin{bmatrix} A & B \end{bmatrix} = \mathrm{qr}\left(\begin{bmatrix} \chi_{k|k-1} - K_k^{et} Z_{k|k-1}^{*et} & K_k^{et} S_{R,k} \end{bmatrix}^T\right), \\ S_k = B(1:n,:)^T, \end{cases}$$
$$K_k^{et} = (P_{xy,k|k-1}^{et} / S_{yy,k|k-1}^{etT}) / S_{yy,k|k-1}^{et}. \quad (40)$$

Based on the discussions given above, the ET-SRCKF algorithm with delay measurement can be formative, which is summarized in Algorithm 1 to facilitate implementations.

Algorithm 1 The ET-SRCKF With Delayed Measurements

1: **Initialise:** x_0, $\hat{x}_0$, N, P_0, S_0, Q_0, R_0, n, m, L
2: **for** $k = 1 : N$
3: Evaluate cubature points
$\chi_{i,k-1} = S_{k-1}\xi_i + \hat{x}_{k-1}$,
4: Compute cubature points propagated through the state equation
$\chi_{i,k|k-1}^{*} = f(\chi_{i,k-1})$,
5: Estimate the predicted state
$\hat{x}_{k|k-1} = {}^1\!/_L \sum_{i=1}^{L} \chi_{i,k|k-1}^{*}$,
6: Compute the square-root factor of predicted error covariance matrix
$S_{k|k-1}$ by (24),
7: Compute $\hat{z}_{k-1}$, $S_{zz,k-1}$, $P_{xz,k-1}$ by (26),
8: Estimate the predicted measurement
$\hat{z}_{k|k-1} = {}^1\!/_L \sum_{i=1}^{L} Z_{i,k|k-1}$,
9: Compute the square-root factor
$S_{zz,k|k-1}$ by (29),
10: Compute the cross-covariance
$P_{xz,k|k-1}^{et} = \chi_{k|k-1}(Z_{k|k-1}^{*et})^T$,
11: Compute $\hat{y}_{d,k|k-1}$, $S_{yy,k|k-1}$, $P_{xy,k|k-1}$ by (25),
12: Compute the gain matrix
$K_k^{et} = (P_{xy,k|k-1}^{et} / S_{yy,k|k-1}^{etT}) / S_{yy,k|k-1}^{et}$,
and provide $\hat{x}_k$, S_k by (40),
14: **end**

IV. Numerical Examples

In this section, the ET-SRCKF based state estimation with delayed measurements is tested in the case study of the IEEE 33-bus test system. To obtain more realistic case studies, the measurement data used in the simulation are obtained by adding white Gaussian noise into the results of power flow. The power flow is calculated by MATPOWER package [42], The standard deviation of SCADA measurement is set to 0.02. The standard deviations of PMU voltage amplitude and phase angle are set to be 0.005 and 0.002 [43], respectively. Furthermore, assume that the initial voltages of all buses are at flat start, that is, $x_{l,0,re} = 1$ p.u, $x_{l,0,im} = 0$ for all $l = \{1, 2, \ldots, 33\}$.

Measuring terminals include traditional DRTUs and PMUs. In Holt's method, the smoothing parameters α_H and β_H are very important for the accuracy of the state prediction model.

TABLE I
MSE of CKF, SRCKF and ET-SRCKF for State Variable

Algorithm	MSE of Amplitude	MSE of Phase angle
CKF	$9.6920e-04$	0.0070
SRCKF	$1.1862e-04$	$5.7329e-06$
ET-SRCKF	$3.2336e-07$	$3.9934e-07$

According to the constraint condition of $\alpha_H(1+\beta_H) < 1$ in [14], we conduct some comparative experiments under different α_H and β_H. As shown in Fig. 3, it can be seen that the algorithm has the best dynamic performance and estimation accuracy when $\alpha_H = 0.8$ and $\beta_H = 0.1$.

1) Voltage magnitude obtained at bus 1.
2) Power injections at buses 2, 3, 7, 8, 10, 11, 12, and 14.
3) Power flows between buses 6-7, 8-9, 13-14, 24-28, and 32-32.

PMUs are separately installed at critical nodes 2, 6, 12, 18, 22, and 33 [44], which can obtain the voltage and current measurements on these nodes. In addition, the corresponding measurement error covariances are $R_{drtu}(k) = \mathrm{diag}_{20}\{0.01\}$, $R_{pmu}(k) = \mathrm{diag}_{36}\{0.01^2\}$ and $W_(k) = \mathrm{diag}_{28}\{0.01^2\}$ [45]. Then, the equivalent measurements error covariance is obtained from Eq. (9). In this section, the main experiments conducted in this test system are classified into three categories.

1) The transmission process of SRCKF algorithm based on event-triggered mechanism under different thresholds is simulated.
2) The comparative experiment of the CKF, SRCKF and proposed ET-SRCKF is implemented.
3) The ET-SRCKF-based state estimation with delayed measurements is compared with various measurement delay rates.

Remark 5: The measurement error covariance matrix represents the uncertainty or variability in a measurement. Different choices of measurement error covariance can have an impact on the performance and results of the ET-SRCKF. A larger measurement error covariance implies a greater uncertainty in the measurement, so we generally assign a smaller measurement error covariance, where the values are set based on previous experience and identical to [45] and [46].

Remark 6: In CPDSs, the most important basis for selecting the location of PMUs is to ensure system observability. However, achieving system observability by increasing the number of measurement devices seems to be economically impossible. Therefore, it is necessary to reduce the number of PMUs installed. We consider installing PMUs only at the beginning and end of the busbars and connections [47], [48], [49].

Due to space constraints, only buses 5 and 7 in the entire IEEE 33-bus system are selected to be the representative buses. Fig. 4 and Fig. 5 respectively show

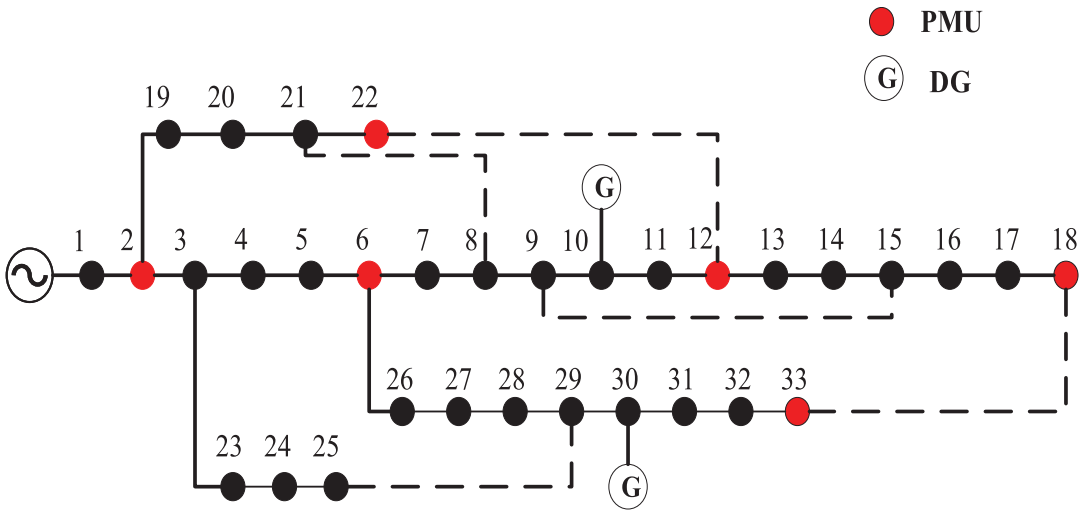

Fig. 2. IEEE 33 bus test system.

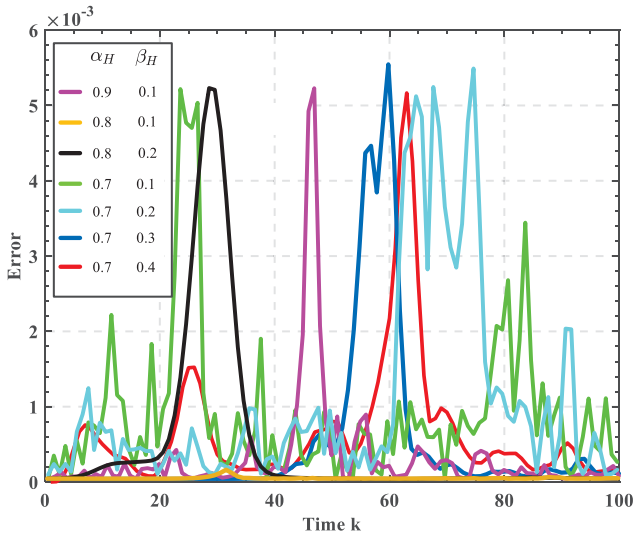

Fig. 3. The estimated error results under different parameters α_H and β_H.

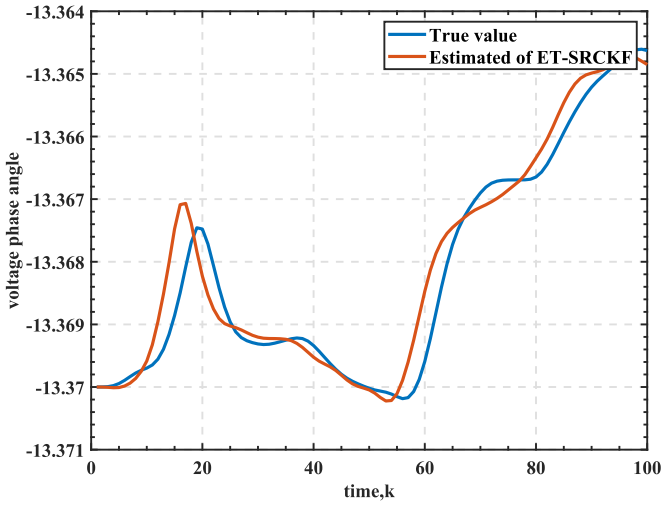

Fig. 4. Estimation of the system attacked.

the actual state and estimated state obtained by ET-SRCKF algorithm under the FDIAs. The results show that the proposed ET-SRCKF algorithm is effective in state estimation.

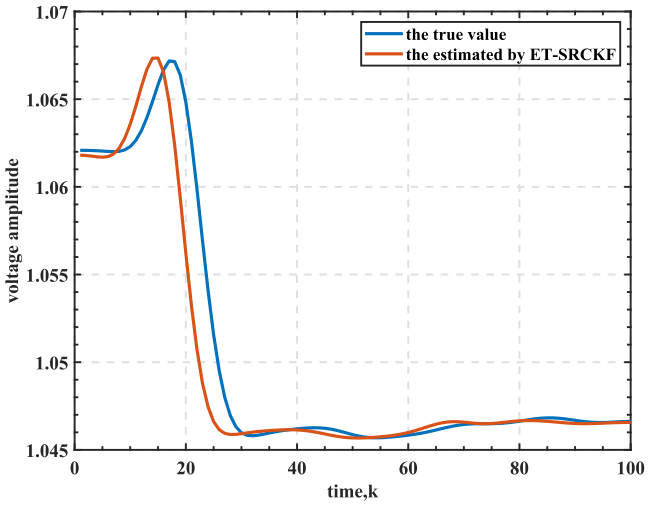

Fig. 5. Estimation of the system attacked.

In order to demonstrate the performance of the event-triggered mechanism, a data transmission ratio (DTR) is defined as a transmission performance index by

$$J_{dtr} = \frac{1}{mk_{\max}} \sum_{j=1}^{j=m} \sum_{k=1}^{k=k_{\max}} \gamma_{j,k} \times 100\%$$

Fig. 6 and Fig. 7 shows the event-triggered instants and event-triggered data transmission rate for an event-triggered threshold $\delta_i = 5 \times 10^{-3}$. It can be seen that the inclusion of the event-triggered transfer mechanism reduces the amount of data transferred from the measurement device to the estimator by approximately 30%.

In order to figure out the impact of various triggering thresholds on estimation performance, simulations are conducted with $\delta_i = 2 \times 10^{-3}$, $\delta_i = 4 \times 10^{-3}$, and $\delta_i = 6 \times 10^{-3}$, respectively. Fig. 8 shows the RMSE of estimation results and DTR with different triggering thresholds. Fig. 9 shows the event-triggering instant with different event-triggering thresholds. It can be found out from these figures that the DTR decreases sharply with the increase in the triggering threshold, which is because the large triggering threshold prevented more measurement

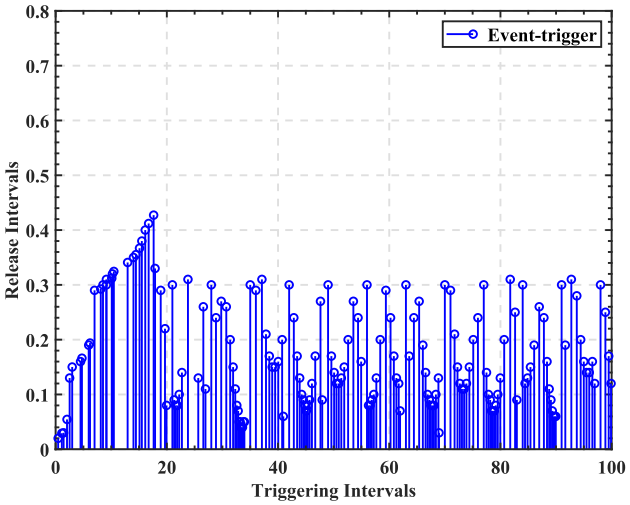

Fig. 6. Event-triggered instants with $\delta_i = 5 \times 10^{-3}$.

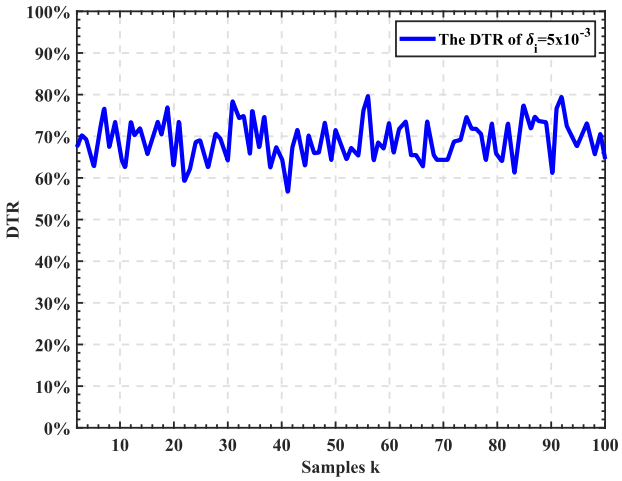

Fig. 7. Data transfer rate under event-triggered mechanism.

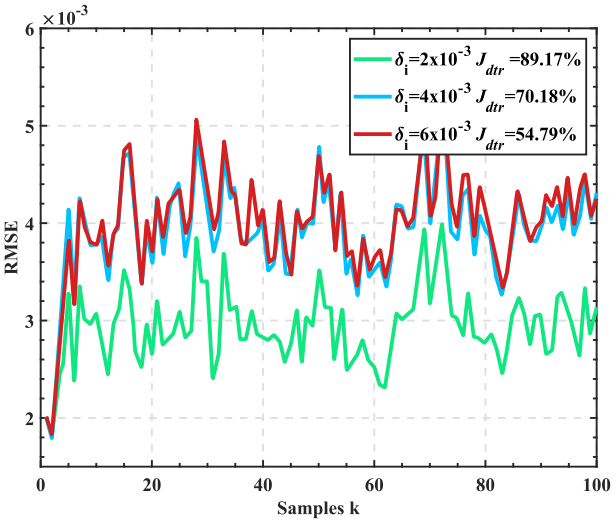

Fig. 8. Variation of the RMSE and J_{dtr} with the trigger threshold.

data from being transmitted to the remote estimation center, suggesting that the event-triggered mechanism contributes to reducing data transmission in the communication network and alleviating the communication pressure.

Remark 7: It can be seen through Fig. 8 and Fig. 9 that when $\delta_i = 2 \times 10^{-3}$, $J_{dtr} = 89.17\%$; when $\delta_i = 4 \times 10^{-3}$, $J_{dtr} = 70.18\%$; when $\delta_i = 6 \times 10^{-3}$, $J_{dtr} = 54.19\%$; as the trigger threshold δ_i increases, J_{dtr} decreases and the RMSE of the estimated results of the ET-SRCKF algorithm increases, which means that the smaller the δ_i, the better the performance of event-triggered mechanism. Therefore, choosing the right threshold in a practical CPDSs can effectively relieve the communication pressure and ensure the performance of state estimation.

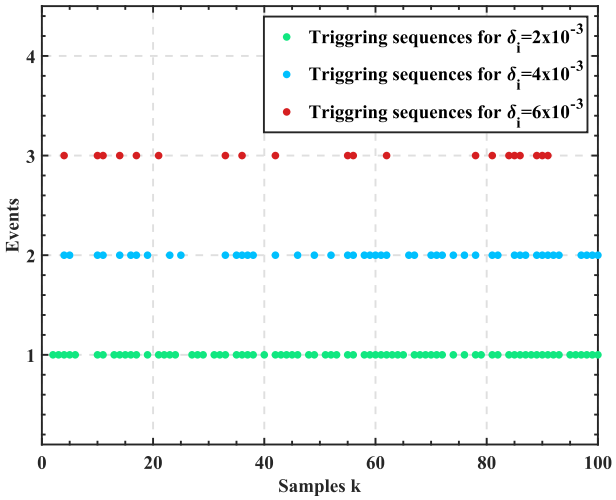

Fig. 9. Event-triggered instants.

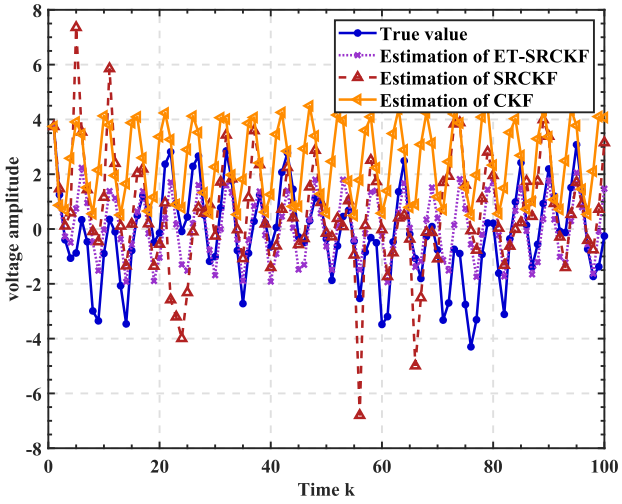

Fig. 10. Estimation result of voltage amplitude.

Fig. 10 and Fig. 11 shows the state tracking curves for the voltage magnitudes and voltage phase angles. As can be seen from the figures, the ET-SRCKF algorithm is able to track changes in the system state and make accurate estimates in real time even when only partial measurements are received, thanks to the fact that the ET-SRCKF algorithm handles non-trigger errors well. Furthermore, it can be clearly seen from Fig. 12 and Fig. 13 that the proposed ET-SRCKF algorithm has better performance for state estimation of CPDSs with delayed mensurements than the SRCKF algorithm and the CKF algorithm.

Fig. 14 shows the errors of the ET-SRCKF algorithm under FDIAs. It can be seen that the ET-SRCKF algorithm has a relatively small error under FDIAs. In order to further compare the performance of CKF, SRCKF and ET-SRCKF

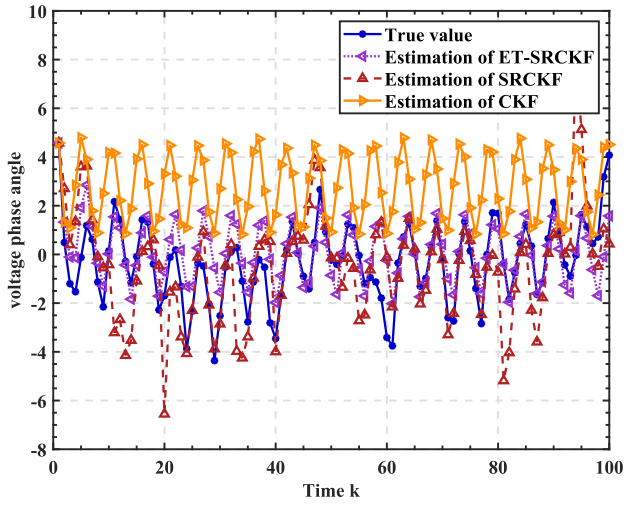

Fig. 11. Estimation result of voltage phase angle.

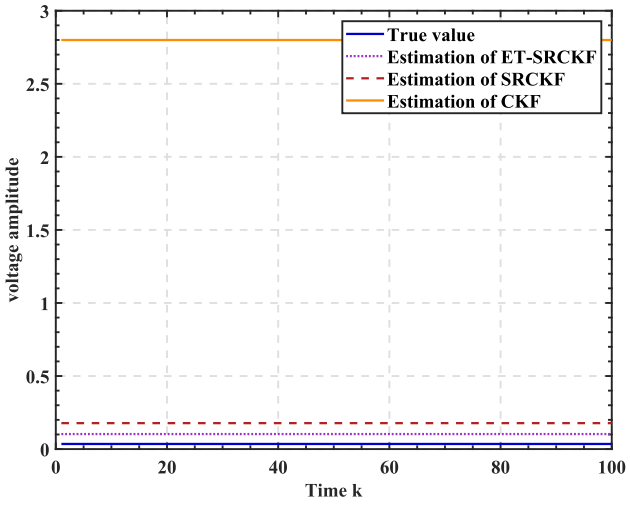

Fig. 12. Estimation result of voltage phase angle.

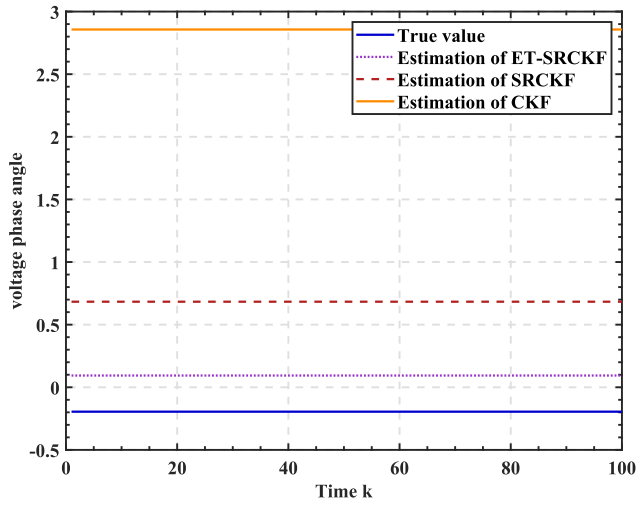

Fig. 13. Estimation result of voltage phase angle.

algorithms, mean square error (MSE) of the state variable is used as the evaluation index, which is defined as follows: $\mathrm{MSE}_k = {}^1\!/_n \sum_{i=1}^{n} (x_k - \hat{x}_k)^2$. The results, listed in Table I, also indicates the effectiveness of the proposed algorithm quantitatively.

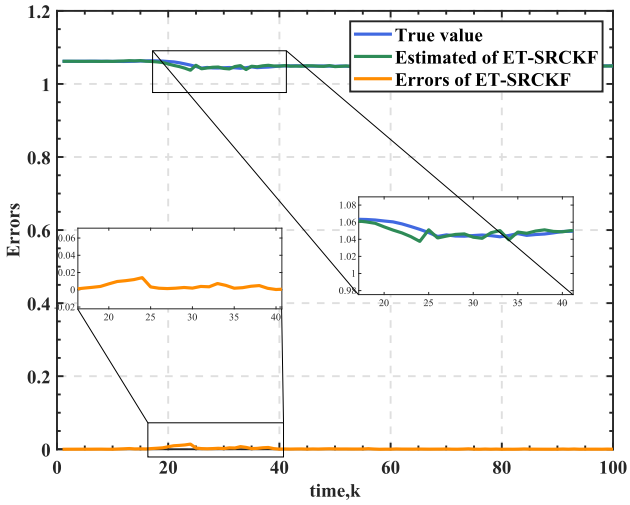

Fig. 14. Estimation errors.

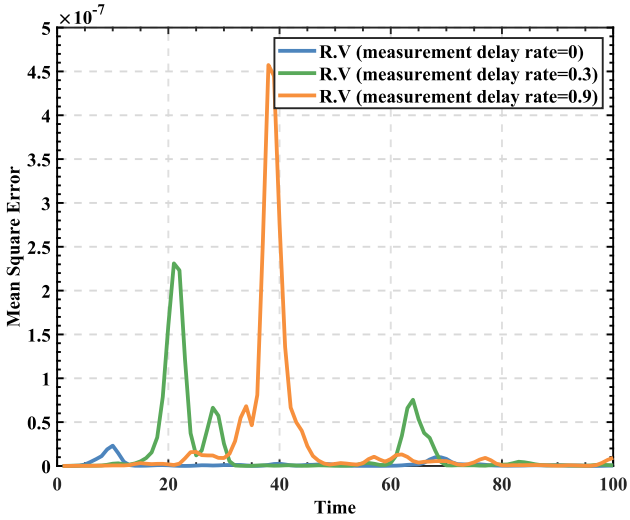

Fig. 15. MSEs of estimated values of real parts of states at bus 5 under various measurement delay rates.

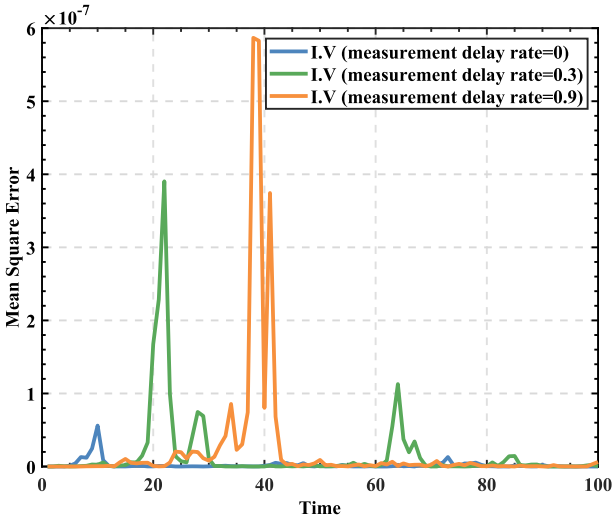

Fig. 16. MSEs of estimated values of imaginary parts of states at bus 5 under various measurement delay rates.

To analyze the impacts of delayed measurements on the CPDSs state estimation, different measurement delay rates are simulated. The MSE used can more accurately describe the accuracy of state estimation. Fig. 15 and Fig. 16 show

the results of state estimation under different measurement delay probabilities, where R.V and I.V represent the real and imaginary parts of the estimated state vector at bus 5, respectively. It can be found that when the measurement delay rate is 0, the waveform is stable; when the measurement delay rate is 0.9, the error deviates from the equilibrium point seriously, and the addressed system oscillates seriously.

V. Conclusion

This work has focused on the problem of dynamic state estimation for measurements with delays. In this paper, in order to cope with the delay phenomenon caused by the transmission of large amount of measurement data in CPDSs, a reliable event-triggered SRCKF method has been proposed, which utilized the event-triggered mechanism to reasonably reduce the redundant transmission. To ensure the state estimation performance under the event-triggered mechanism, the ET-SRCKF algorithm has designed. Finally, the effectiveness of the method has verified by simulation. In view of the importance of the new power system as a development trend in the new energy field, the development of high-performance state estimation algorithms for the new power system has become an urgent task, and future research will consider the dynamic characteristics of different systems in the integrated energy system and apply the algorithms proposed in this study to the new power system.

References

[1] M. Hammoudeh, G. Epiphaniou, and P. Pinto, "Cyber-physical systems: Security threats and countermeasures," *J. Sensor Actuator Netw.*, vol. 12, no. 1, p. 18, Feb. 2023.

[2] W. Duo, M. Zhou, and A. Abusorrah, "A survey of cyber attacks on cyber physical systems: Recent advances and challenges," *IEEE/CAA J. Autom. Sinica*, vol. 9, no. 5, pp. 784–800, May 2022.

[3] Z. Zhao and Y. Xu, "Performance based attack detection and security analysis for cyber-physical systems," *Int. J. Robust Nonlinear Control*, vol. 33, no. 5, pp. 3267–3284, 2023.

[4] E. Vincent, M. Korki, M. Seyedmahmoudian, A. Stojcevski, and S. Mekhilef, "Detection of false data injection attacks in cyber–physical systems using graph convolutional network," *Electric Power Syst. Res.*, vol. 217, Apr. 2023, Art. no. 109118.

[5] W. Qi, Y. Hou, G. Zong, and C. K. Ahn, "Finite-time event-triggered control for semi-Markovian switching cyber-physical systems with FDI attacks and applications," *IEEE Trans. Circuits Syst. I, Reg. Papers*, vol. 68, no. 6, pp. 2665–2674, Jun. 2021.

[6] R. Wang, Q. Sun, H. Zhang, L. Liu, Y. Gui, and P. Wang, "Stability-oriented minimum switching/sampling frequency for cyber-physical systems: Grid-connected inverters under weak grid," *IEEE Trans. Circuits Syst. I, Reg. Papers*, vol. 69, no. 2, pp. 946–955, Feb. 2022.

[7] S. Hampannavar, M. Swapna, B. Deepa, and U. Yaragatti, "Micro phasor measurement unit (μPMU) in smart distribution network: A cyber physical system," in *Proc. Int. Conf. Intell. Cyber-Phys. Syst.*, 2021, pp. 1–10.

[8] G. Zeng, T. Yu, Z. Wang, and D. Lin, "Analytical reliability assessment of cyber-physical distribution system with distributed feeder automation," *Electric Power Syst. Res.*, vol. 208, Jul. 2022, Art. no. 107864.

[9] F. U. Din, A. Ahmad, H. Ullah, A. Khan, T. Umer, and S. Wan, "Efficient sizing and placement of distributed generators in cyber-physical power systems," *J. Syst. Archit.*, vol. 97, pp. 197–207, Aug. 2019.

[10] M. K. Hasan, A. A. Habib, Z. Shukur, F. Ibrahim, S. Islam, and M. A. Razzaque, "Review on cyber-physical and cyber-security system in smart grid: Standards, protocols, constraints, and recommendations," *J. Netw. Comput. Appl.*, vol. 209, Jan. 2023, Art. no. 103540.

[11] J. Qin, M. Li, J. Wang, L. Shi, Y. Kang, and W. X. Zheng, "Optimal denial-of-service attack energy management against state estimation over an SINR-based network," *Automatica*, vol. 119, Sep. 2020, Art. no. 109090.

[12] H. Ren, R. Lu, J. Xiong, Y. Wu, and P. Shi, "Optimal filtered and smoothed estimators for discrete-time linear systems with multiple packet dropouts under Markovian communication constraints," *IEEE Trans. Cybern.*, vol. 50, no. 9, pp. 4169–4181, Sep. 2020.

[13] S. Li et al., "Stochastic event-triggered cubature Kalman filter for power system dynamic state estimation," *IEEE Trans. Circuits Syst. II, Exp. Briefs*, vol. 66, no. 9, pp. 1552–1556, Sep. 2019.

[14] C. Cheng and X. Bai, "Robust forecasting-aided state estimation in power distribution systems with event-triggered transmission and reduced mixed measurements," *IEEE Trans. Power Syst.*, vol. 38, no. 5, pp. 4343–4354, Sep. 2021.

[15] L. Hu, Z. Wang, X. Liu, A. V. Vasilakos, and F. E. Alsaadi, "Recent advances on state estimation for power grids with unconventional measurements," *IET Control Theory Appl.*, vol. 11, no. 18, pp. 3221–3232, Dec. 2017.

[16] L. Hu, Z. Wang, and X. Liu, "Dynamic state estimation of power systems with quantization effects: A recursive filter approach," *IEEE Trans. Neural Netw. Learn. Syst.*, vol. 27, no. 8, pp. 1604–1614, Aug. 2016.

[17] J. Zhao and L. Mili, "A framework for robust hybrid state estimation with unknown measurement noise statistics," *IEEE Trans. Ind. Informat.*, vol. 14, no. 5, pp. 1866–1875, May 2018.

[18] Z. Cheng, H. Ren, B. Zhang, and R. Lu, "Distributed Kalman filter for large-scale power systems with state inequality constraints," *IEEE Trans. Ind. Electron.*, vol. 68, no. 7, pp. 6238–6247, Jul. 2021.

[19] J. Xu, Z. Wu, X. Yu, and C. Zhu, "Robust faulted line identification in power distribution networks via hybrid state estimator," *IEEE Trans. Ind. Informat.*, vol. 15, no. 9, pp. 5365–5377, Sep. 2019.

[20] S. Obata, K. Kobayashi, and Y. Yamashita, "Sensor scheduling-based detection of false data injection attacks in power system state estimation," *IEICE Trans. Fundam. Electron., Commun. Comput. Sci.*, vol. 105, no. 6, pp. 1015–1019, 2022.

[21] W. Wang, C. K. Tse, and S. Wang, "Dynamic state estimation of power systems by p-norm nonlinear Kalman filter," *IEEE Trans. Circuits Syst. I, Reg. Papers*, vol. 67, no. 5, pp. 1715–1728, May 2020.

[22] H. Zhang, B. Liu, and H. Wu, "Smart grid cyber-physical attack and defense: A review," *IEEE Access*, vol. 9, pp. 29641–29659, 2021.

[23] N. Pang, Y. Luo, and Y. Zhu, "A novel model for linear dynamic system with random delays," *Automatica*, vol. 99, pp. 346–351, Jan. 2019.

[24] V. T. Huynh, A. Arogbonlo, H. Trinh, and A. M. T. Oo, "Design of observers for positive systems with delayed input and output information," *IEEE Trans. Circuits Syst. II, Exp. Briefs*, vol. 67, no. 1, pp. 107–111, Jan. 2020.

[25] Z. Yu, Y. Sun, and X. Dai, "Stability and stabilization of the fractional-order power system with time delay," *IEEE Trans. Circuits Syst. II, Exp. Briefs*, vol. 68, no. 11, pp. 3446–3450, Nov. 2021.

[26] J. Hu, Z. Wang, and G.-P. Liu, "Delay compensation-based state estimation for time-varying complex networks with incomplete observations and dynamical bias," *IEEE Trans. Cybern.*, vol. 52, no. 11, pp. 12071–12083, Nov. 2022.

[27] I. Mohammed, S. J. Geetha, S. S. Shinde, K. Rajawat, and S. Chakrabarti, "Modified re-iterated Kalman filter for handling delayed and lost measurements in power system state estimation," *IEEE Sensors J.*, vol. 20, no. 7, pp. 3946–3955, Apr. 2020.

[28] Z. Wang, Y. Huang, Y. Zhang, G. Jia, and J. Chambers, "An improved Kalman filter with adaptive estimate of latency probability," *IEEE Trans. Circuits Syst. II, Exp. Briefs*, vol. 67, no. 10, pp. 2259–2263, Oct. 2020.

[29] Y. Wei, J. Qiu, H. R. Karimi, and W. Ji, "A novel memory filtering design for semi-Markovian jump time-delay systems," *IEEE Trans. Syst., Man, Cybern., Syst.*, vol. 48, no. 12, pp. 2229–2241, Dec. 2018.

[30] C. L. Su and C. N. Lu, "Interconnected network state estimation using randomly delayed measurements," *IEEE Trans. Power Syst.*, vol. 16, no. 4, pp. 870–878, Nov. 2001.

[31] A. Nikfetrat and R. M. Esfanjani, "Adaptive Kalman filtering for systems subject to randomly delayed and lost measurements," *Circuits, Syst., Signal Process.*, vol. 37, no. 6, pp. 2433–2449, Jun. 2018.

[32] P. Yang, Z. Tan, A. Wiesel, and A. Nehorai, "Power system state estimation using PMUs with imperfect synchronization," *IEEE Trans. Power Syst.*, vol. 28, no. 4, pp. 4162–4172, Nov. 2013.

[33] J. Hu, C. Jia, H. Liu, X. Yi, and Y. Liu, "A survey on state estimation of complex dynamical networks," *Int. J. Syst. Sci.*, vol. 52, no. 16, pp. 3351–3367, Dec. 2021.

[34] I. Zografopoulos, J. Ospina, X. Liu, and C. Konstantinou, "Cyber-physical energy systems security: Threat modeling, risk assessment, resources, metrics, and case studies," *IEEE Access*, vol. 9, pp. 29775–29818, 2021.
[35] W. Song, J. Wang, S. Zhao, and J. Shan, "Event-triggered cooperative unscented Kalman filtering and its application in multi-UAV systems," *Automatica*, vol. 105, pp. 264–273, Jul. 2019.
[36] M. Kooshkbaghi, H. J. Marquez, and W. Xu, "Event-triggered approach to dynamic state estimation of a synchronous machine using cubature Kalman filter," *IEEE Trans. Control Syst. Technol.*, vol. 28, no. 5, pp. 2013–2020, Sep. 2020.
[37] R. Meng, C. Hua, K. Li, and P. Ning, "Dynamic event-triggered control for nonlinear stochastic systems with unknown measurement sensitivity," *IEEE Trans. Circuits Syst. I, Reg. Papers*, vol. 70, no. 4, pp. 1710–1719, Apr. 2023.
[38] N. Zhao, P. Shi, W. Xing, and C. P. Lim, "Event-triggered control for networked systems under denial of service attacks and applications," *IEEE Trans. Circuits Syst. I, Reg. Papers*, vol. 69, no. 2, pp. 811–820, Feb. 2022.
[39] J. Linares-Pérez, A. Hermoso-Carazo, R. Caballero-Águila, and J. D. Jiménez-López, "Least-squares linear filtering using observations coming from multiple sensors with one- or two-step random delay," *Signal Process.*, vol. 89, no. 10, pp. 2045–2052, Oct. 2009.
[40] Y. Zhang and X. Mus, "Event-triggered output quantized control of discrete Markovian singular systems," *Automatica*, vol. 135, Jan. 2022, Art. no. 109992.
[41] Y. Zhang, P. Shi, R. K. Agarwal, and Y. Shi, "Event-based dissipative analysis for discrete time-delay singular jump neural networks," *IEEE Trans. Neural Netw. Learn. Syst.*, vol. 31, no. 4, pp. 1232–1241, Apr. 2020.
[42] R. D. Zimmerman, C. E. Murillo-Sánchez, and R. J. Thomas, "MATPOWER: Steady-state operations, planning, and analysis tools for power systems research and education," *IEEE Trans. Power Syst.*, vol. 26, no. 1, pp. 12–19, Feb. 2011.
[43] Y. Wang, M. Xia, Q. Yang, Y. Song, Q. Chen, and Y. Chen, "Augmented state estimation of line parameters in active power distribution systems with phasor measurement units," *IEEE Trans. Power Del.*, vol. 37, no. 5, pp. 3835–3845, Oct. 2022.
[44] J. Li, M. Gao, B. Liu, and Y. Cai, "Forecasting aided distribution network state estimation using mixed μPMU-RTU measurements," *IEEE Syst. J.*, vol. 16, no. 4, pp. 6524–6534, Dec. 2022.
[45] L. Hu, Z. Wang, I. Rahman, and X. Liu, "A constrained optimization approach to dynamic state estimation for power systems including PMU measurements and missing measurements," *IEEE IEEE Trans. Control Syst. Technol.*, vol. 24, no. 2, pp. 703–710, Mar. 2016.
[46] Z. Cheng, H. Ren, J. Qin, and R. Lu, "Security analysis for dynamic state estimation of power systems with measurement delays," *IEEE Trans. Cybern.*, vol. 53, no. 4, pp. 2087–2096, Apr. 2023.
[47] P. Yang, Z. Tan, A. Wiesel, and A. Nehorai, "Placement of PMUs considering measurement phase-angle mismatch," *IEEE Trans. Power Del.*, vol. 30, no. 2, pp. 914–922, Apr. 2015.
[48] H. Su, C. Wang, P. Li, Z. Liu, L. Yu, and J. Wu, "Optimal placement of phasor measurement unit in distribution networks considering the changes in topology," *Appl. Energy*, vol. 250, pp. 313–322, Sep. 2019.
[49] V. L. Srinivas and J. Wu, "Topology and parameter identification of distribution network using smart meter and μPMU measurements," *IEEE Trans. Instrum. Meas.*, vol. 71, pp. 1–14, 2022.

Xiao Hu (Graduate Student Member, IEEE) received the B.S. degree in automation from Hubei Normal University of Mechatronics and Control Engineering, Huangshi, China, in 2022. He is currently pursuing the Ph.D. degree in electric engineering with Xi'an University of Technology, Xi'an, China. His current research interests include networked control systems, cyber-physical systems, and power system dynamic state estimation.

Xinghua Liu (Senior Member, IEEE) received the B.Sc. degree from Jilin University, Changchun, China, in 2009, and the Ph.D. degree in automation from the University of Science and Technology of China, Hefei, in 2014. From 2014 to 2015, he was invited as a Visiting Fellow with RMIT University, Melbourne, Australia. From 2015 to 2018, he was a Research Fellow with the School of Electrical and Electronic Engineering, Nanyang Technological University, Singapore. He has been with Xi'an University of Technology as a Professor since September 2018. His research interests include state estimation and control, intelligent systems, autonomous vehicles, cyber-physical systems, and robotic systems.

Huaicheng Yan (Senior Member, IEEE) received the B.Sc. degree in automatic control from Wuhan University of Technology, Wuhan, China, in 2001, and the Ph.D. degree in control theory and control engineering from Huazhong University of Science and Technology, Wuhan, in 2007. In 2011, he was a Research Fellow with The University of Hong Kong, Hong Kong, for three months. In 2012, he was a Research Fellow with the City University of Hong Kong, Hong Kong, for six months. He is currently a Professor with the School of Information Science and Engineering, East China University of Science and Technology, Shanghai, China. His research interests include networked control systems, multi-agent systems, and robotics. He is an Associate Editor of IEEE TRANSACTIONS ON NEURAL NETWORKS AND LEARNING SYSTEMS, IEEE TRANSACTIONS ON FUZZY SYSTEMS, *International Journal of Robotics and Automation*, and IEEE OPEN JOURNAL OF CIRCUITS AND SYSTEMS.

Gaoxi Xiao (Senior Member, IEEE) received the B.S. and M.S. degrees in applied mathematics from Xidian University, Xi'an, China, in 1991 and 1994, respectively, and the Ph.D. degree in computing from The Hong Kong Polytechnic University, Hong Kong, in 1998. He was an Assistant Lecturer with Xidian University from 1994 to 1995. He was a Post-Doctoral Research Fellow with Polytechnic University, Brooklyn, NY, USA, in 1999, and a Visiting Scientist with The University of Texas at Dallas, Richardson, TX, USA, from 1999 to 2001. He joined the School of Electrical and Electronic Engineering, Nanyang Technological University, Singapore, in 2001, where he is currently an Associate Professor. His current research interests include complex systems and complex networks, communication networks, smart grids, and system resilience and risk management. He is a TPC Member for numerous conferences, including the IEEE ICC and the IEEE GLOBECOM. He serves/served as an Editor or the Guest Editor for IEEE TRANSACTIONS ON NETWORK SCIENCE AND ENGINEERING, *PLOS One*, and *Advances in Complex Systems*.

Peng Wang (Fellow, IEEE) received the B.Sc. degree in electrical engineering from Xi'an Jiaotong University, Xi'an, China, in 1978, the M.Sc. degree in electrical engineering from the Taiyuan University of Technology, Taiyuan, China, in 1987, and the M.Sc. and Ph.D. degrees in electrical engineering from the University of Saskatchewan, Saskatoon, SK, Canada, in 1995 and 1998, respectively. He is currently a Professor with Nanyang Technological University, Singapore. His research interests include power system planning and operation, renewable energy planning, solar/electricity conversion systems, and power system reliability analysis. He served as an Associate Editor for IEEE TRANSACTIONS ON SMART GRID and the Guest Editor for *Journal of Modern Power Systems and Clean Energy* Special Issues on smart grids. He also served as an Associate Editor for IEEE TRANSACTIONS ON POWER DELIVERY and the Guest Editor-in-Chief for *CSEE Journal of Power and Energy Systems* Special Issues on hybrid AC/DC grids for future power systems.